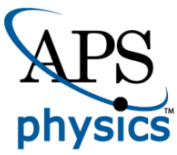

Dynamics of Single-Molecule Dissociation by Selective Excitation of Molecular Phonons

Caiyun Chen, Longjuan Kong, Yu Wang, Peng Cheng, Baojie Feng, Qijing Zheng, Jin Zhao, Lan Chen, and Kehui Wu

Phys. Rev. Lett. **123**, 246804 — Published 13 December 2019

DOI: 10.1103/PhysRevLett.123.246804

Dynamics of single-molecule dissociation by selective excitation of molecular phonons

Caiyun Chen[1,3#], Longjuan Kong[1,3#], Yu Wang[1,3], Peng Cheng[1,3], Baojie Feng[1], Qijing Zheng[2], Jin Zhao[2,5]*, Lan Chen[1, 3, 4]*, Kehui Wu[1, 3, 4]

[1]*Institute of Physics, Chinese Academy of Sciences, Beijing 100190, China*

[2]*ICQD/Hefei National Laboratory for Physical Sciences at Microscale, and Key Laboratory of Strongly-Coupled Quantum Matter Physics, Chinese Academy of Sciences, and Department of Physics, University of Science and Technology of China, Hefei, Anhui 230026, China*

[3]*School of physics, University of Chinese Academy of Sciences, Beijing 100049, China*

[4]*Songshan Lake Materials Laboratory, Dongguan, Guangdong 523808, China*

[5]*Synergetic Innovation Center of Quantum Information & Quantum Physics, University of Science and Technology of China, Hefei, Anhui 230026, China*

*Email: lchen@iphy.ac.cn (L. C.) and zhaojin@ustc.edu.cn (J. Z.)

[#]these authors contributed equally to this work.

Abstract: Breaking bonds selectively in molecules is vital in many chemistry reactions and custom nanoscale device fabrication. The scanning tunneling microscope (STM) has been proven to be an ideal tool to initiate and view bond-selective chemistry at the single-molecule level, offering opportunities for the further study of the dynamics in single molecules on metal surfaces. Here, we demonstrate H-HS and H-S bond breaking on Au(111) induced by tunneling electrons using low-temperature STM. The experimental study combined with theoretical calculations shows that the dissociation pathway is facilitated by vibrational excitations**.** Furthermore, the dissociation probabilities of the two different dissociation processes are bias-dependent due to different inelastical tunneling probabilities, and are also closely linked to the lifetime of inelastic tunneling electrons. Combined with time-dependent *ab initio* nonadiabatic molecular dynamics simulations, the dynamics of the injected electron and the phonon excitation induced molecule dissociation can be understood at the atomic scale, demonstrating the potential application of STM for the investigation of excited state dynamics of single molecules on surfaces.

The excitation of molecular vibrations, e.g. the phonons, plays an important role in various surface dynamic phenomena [1-9], for example, in molecular dissociation [9-11]. It can help the molecules overcome the activation barrier for chemical bond cleaving [12-15]. The scanning tunneling microscopy (STM) is a powerful technique for investigating chemical reactions on surfaces through initiating electronic and vibrational excitations in molecules by inelastic-tunneling (IET) electrons [9, 10, 16-22]. By controlling the energy and injection location of inelastic-electrons, mode-selective chemical reactions on surfaces can be achieved by STM with high spatial and energy resolutions [21, 23-25], perfect for studying single-molecule reactions on surface.

Most previous STM studies did not probe the dynamics of inelastic electron relaxations, phonon excitations and surface chemical reactions, because STM is generally used to measure the static atomic and electronic structures. Nevertheless, the outcome of the chemical reactions has strong correlation with the coherence dynamics of atoms and electrons. STM is able to estimate and regulate the femtosecond (fs) lifetime of excited electrons on single molecules [22, 26], suggesting its capability of controlling single molecule dynamics on surfaces. Yet, only a simple empirical model was previously used to estimate the lifetime of excited states in the molecule. The comprehensive dynamics incorporating the chemical reaction with femtosecond time resolution is still challenging to model.

In this report, we study inelastic-electron-induced molecule dissociation of H_2S on a Au(111) surface by combining the STM with time-resolved nonadiabatic molecular dynamics (NAMD) within the framework of the time-dependent Kohn-Sham equation (TDKS) [27]. The H_2S molecule was chosen because H_2S and its dissociation products have played an important role in electrochemistry, corrosion, environmental chemistry, and heterogeneous catalysis [43-45].

The H_2S molecules physically adsorb on Au(111) [46-50], so we only resolve individual H_2S molecules by STM at LHe temperature. Figure 1(a) is a large-area STM image of 0.01 monolayer H_2S molecules adsorbed on Au(111) at 4.7 K. Individual H_2S molecules on Au(111) appear as rounded protrusions in high-resolution images [Fig. 1(b)] and the apparent height is about 130 pm. The optimum configuration of an isolated H_2S molecule on Au(111) from DFT calculations [Fig. 1(d)] indicate the H_2S monomer adsorbs flat with the S atom located atop a Au atom. The distances between S and Au atom is 2.67 Å corresponding to an adsorption energy -0.5 eV, suggesting a relatively weak molecule-surface interaction.

Applying a pulse (-1.0 V, 0.8 nA, 100 ms) on the target H_2S molecule [label as A in Fig. 1(b)], changes it to a ball-shaped and darker protrusion [A' in Fig. 1(c)], with height of about 65 pm. By continuing to apply another pulse on the reacted molecule, a much darker dot with height of 7 pm was obtained [B' in Fig. 1(c)]. Because of the simple stoichiometric ratio of H_2S molecule, we postulate that the chemical reactions induced by STM pulses are the dissociation of H_2S, and dissociation of HS respectively, and the reaction products are HS molecule and S atom, respectively.

DFT calculation result of HS on Au(111) is shown in Fig. 1(e), indicating the S atom in HS prefers to adsorb on the bridge site. The adsorption energy of HS is -2.16 eV, which is much stronger than H_2S on Au(111). The optimized distance between the S atom and Au atom is 2.50 Å. Moreover, S atom is energetically favorable on the hollow-fcc adsorption site [Fig. 1(f)]. The corresponding simulated STM images of H_2S, HS and S on Au(111) are shown in Fig. 1(d-f) and Fig. S3 [27], indicating the similar protrusions as experimental images. Furthermore, the line profiles along H_2S, HS molecule and S atom shown in Fig. 1(g, h) and Fig. S3 [27], reflect the height evolution from H_2S to S in both experimental measurements and theoretical simulations can agree with each other qualitatively, suggesting that our proposed reacted products are reasonable. Similar DFT investigations for H_2S, HS and S were previously reported [47-49].

To find out the dissociation reaction mechanism, we statistically analyzed the dissociation probability (in our experiments, the dissociation probability is defined as ratio of the number of reaction events to the number of applied pulses (> 100 times) with same energy, current and duration time), as shown in Fig. 2. The energy onsets for the H_2S->HS dissociation reactions on Au(111) are determined to be -0.33 eV (electrons from tip to surface) and 0.35 eV (electrons from surface to tip), while the energy onsets for HS->S dissociation are -0.38 and 1.25 eV, respectively. The similar relative low energy onsets suggest the same mechanism for both dissociation reactions. However, the dissociation probability induced by positive pulses is clearly lower than negative pulses, which might result from the different origins of tunneling electrons (i.e. electrons emitted from tip or from substrate). The screening effect of the substrate leads to a decreasing IET probability, and consequently a lower dissociation possibility [51, 52]. The behaviors for these two dissociation reactions are different. For the H_2S->HS dissociation, when the pulse energy is higher than the threshold, the dissociation probabilities increase fast and

are then saturated with energy higher than 1.25 eV [Fig. 2(a)]. For the HS->S dissociation, the dissociation probabilities remain low and increase only with energy larger than 1.25 eV [Fig. 2(b)].

Our experimental results indicate that the chemical bond cleavage in adsorbates is attributed to the injection of tunneling electrons temporarily trapped by the molecular orbitals at molecule/metal interface via an IET process, which can induce molecular dynamical processes such as lateral hopping [3, 5], rotation [1, 2], dissociation [9-11], desorption [23] and single-bond formation [53]. Thus, detailed knowledge of the electronic structures and molecular orbitals at the molecule-substrate interface is instructive for understanding the mechanism of chemical bond cleavage processes for H_2S (HS) on Au(111).

The total and projected density of states (PDOS), together with the spatial distribution of frontier molecular orbitals contributed by isolated H_2S molecule both in gas phase and on the Au (111) surface are shown in Fig. 3 (a). It is apparent that some small electronic states composed of $3p_z$ orbitals of S atom emerge near the Fermi level (E_F) for H_2S molecule on Au(111). For HS adsorbed on Au(111) [Fig. 3(b)], due to the stronger interactions between S and Au atoms, more pronounced hybridization of states occur near E_F. According to the PDOS shown in Fig. 3, the incident electrons with energies between 0.33 and 2.5 eV cannot transfer into the LUMO of H_2S (~3.0 eV) or HS (~3.7 eV) on the Au surface. This implies that the successive H-S bond cleavages are not ascribed to the weakened H-S bonds via electrons transferring to anti-bonding orbitals. Considering the low threshold bias for dissociation reactions (0.33 or 0.38 eV), we postulated that the H-S bond cleavages is associated with vibrational excitations.

To verify this hypothesis, we calculated the phonon modes of H_2S and HS molecules on Au(111), as shown in Fig. 3(c-d). The phonon energies of individual H_2S on Au (111) at 0.328, 0.326 and 0.14 eV correspond to the asymmetric stretch [$\nu_a(H_2S)$], symmetric stretch [$\nu_s(H_2S)$], and bending mode [$\nu_b(H_2S)$], respectively. Similarly, the stretching [ν_s(HS)], perpendicular-to-surface rotation [ν_r(HS)] and bending modes [ν_b(HS)] of adsorbed HS are at 0.32, 0.069 and 0.058 eV, respectively. It is known that, phonon modes of adsorbed molecules can be excited by the IET process [12-15]. The threshold bias 0.33 eV for H_2S dissociation matches the two stretching modes, $\nu_a(H_2S)$ and $\nu_s(H_2S)$ well, while the threshold bias ~0.38 eV for HS dissociation accords with the excitation energy of ν_s(HS) well. The perfect matches indicate that the H_2S and HS bond cleavages are induced by phonon excitation due to energy transfer from IET electrons to the molecules.

The asymmetric and symmetric stretch modes for H_2S on Au(111) have nearly degenerate energies. It is intuitive that the asymmetric stretch mode should induce one H-S bond cleaving, while the symmetric stretch mode induces two H-S bonds cleavage simultaneously. However, in experiments, two H-S bond cleaving reactions were not observed. To elucidate the origin of selectivity for responsible vibration modes, we calculated the energy barriers for molecular dissociations by the climbing-image nudged elastic band (cNEB) method [34]. Two reaction pathways of H-S bond cleavage in H_2S molecule are calculated. The barrier for H_2S–>H+HS process on Au(111) surface is ~0.83 eV [Fig. 4(a)]. For H_2S –> H+H+S, the cNEB calculations are difficult to converge. This reaction tends to happen by breaking the two HS bonds one by one. To estimate the energy barrier, we simultaneously stretch the two HS bonds and allow the molecule to relax in the direction perpendicular to the surface (Fig. S11) [27]. In this way the energy barrier for the simultaneous dissociation is estimated to be 2.31 eV. The much higher energy barrier for two H-S bonds cleaving simultaneously explains why that reaction is not observed in experiments. In addition, as shown in Fig. 4(c-d), the calculated energy barrier for the HS–>H+S process is ~0.89 eV.

Comparing the dissociation barrier (0.83 or 0.89 eV) with the threshold bias 0.33 or 0.38 eV, multiple phonons should be excited to overcome the dissociation barrier. The proposed microscopic picture can be verified by tracing the trajectory of the variation of H-S bond lengths in molecular dynamics (MD) simulation. Our simulations reveal that when four phonons are excited, the lengths of two H-S bonds oscillates for three periods, then one of them elongates gradually leading to single-bond breaking at ~70 fs [Fig. 5(a)]. Fig. 5(b-e) gives the time evolution geometries for H_2S on Au(111) at 35 fs intervals. After 35 fs [Fig. 5(c)], one H atom tilts towards the Au surface and its distance from S is elongated until it breaks away from the HS fragment at 70 fs [Fig. 5(d)]. The case for the dissociation of HS on Au(111) is similar, as shown in Fig. 5(f-j) and Fig. S5(a-c) [27]. The excitation of four phonons is also required for the HS dissociation reaction. The frequencies of different phonon modes can also be obtained from the Fourier transform (FT) spectra from the NAMD simulation, agreeing with static DFT calculations [27]. Based on the potential barrier values estimated by cNEB method, three phonons with energy of 0.33 eV (0.32 eV) for H_2S (HS) are, in principle, sufficient to overcome the reaction barriers for dissociation in a vibrational ladder climbing manner [54]. However, the direction of excited S-H stretching mode by IET electrons is different from reaction coordinate of cNEB and the dynamic behavior of dissociation by

vibrational excitation is not completely the along cNEB path with the lowest energy barrier (Fig. S7 [27]). The dissociated process should involve a higher effective barrier height for four phonons to climb up.

Therefore, we deduce the dissociation pathway of H_2S on Au(111) comprises four phonons with asymmetric stretching modes excited by inelastic electrons. Below the bias of 1.25 eV, more than one electron is needed for the four phonons excitation. The energy of single inelastic electron above 1.25 eV is sufficient to excite four phonons to overcome dissociation barrier, explaining why the dissociation probability is saturated when the pulse bias is larger than ~1.25 eV. The case of HS is similar to H_2S. The variation of probability with bias also indicates that energy transfers from more than one tunneling electron are required to break the H-S bond at low bias. Using equilibrium molecular dynamics simulations and normal mode decomposition [39], the lifetime of the asymmetric stretching mode of H_2S due to anharmonic phonon-phonon interaction is estimated to be 704 fs [27], which is much longer than the timescale of H_2S dissociation, supporting the phonon-induced molecular dissociation postulate. During the dissociation processes of H_2S and HS, due to the anharmonic coupling between different phonon modes, the energy transfers to other modes like Au-S and Au-Au stretching mode. All these modes play a role in the dissociation. However, since the dissociation timescale is much shorter than the phonon lifetime, we think the anharmonic effects within such a short timescale is not significant.

The molecular phonons are excited by IET electrons trapped in hybridized states of molecule near E_F. Therefore, the lifetime of injected electrons in hybridized states will influence the dissociation probability. We employed time-dependent *ab initio* NAMD to elucidate the dynamics of injected electrons in H_2S and HS molecules on Au(111). First, we plotted time-dependent energy evolution of selected states in 2 ps MD at 100 K (Fig. S8 and Fig. S9 [27]). For both H_2S and HS on Au(111), the adiabatic electron-phonon coupling induces the fluctuation of these Kohn-Sham eigen-energies. The lifetime is determined to be the time interval of the electron relaxation from hybridized states to E_F. Figure 6 shows the variation of lifetime with initial energy of injected electrons on H_2S and HS molecules, respectively. The lifetime of electron on HS is always shorter than H_2S by 0.3 to 1.2 eV, and the largest difference occurs at 0.6~0.7 eV. The lifetimes of both H_2S and HS are similar at 0.33 or 1.25 eV, which are close to the threshold and saturation energies for the H_2S dissociation. The stronger hybridization between HS and Au(111) surface generates higher density of states in the relevant energy region (Fig. 3(b) and Fig. S9 [27]). It contributes more efficient cooling channels for excited electron relaxing, and

reduces the lifetime of HS molecule progressing on the excited-state potential energy surface from 0.38 to 1.25 eV. The short-lived travel of HS on excited state cannot provide enough time to accumulate four vibrational modes of ν_s(HS) to overcome the dissociation barrier, explaining the low-value plateaus of dissociation probability for HS [Fig. 2 (b)]. In addition, the higher probability for H_2S dissociation saturates at ~1.25 eV, corresponding to the short lifetime of tunneling electron. By this token, the excited-state lifetime of injected electron and adsorbed molecular dissociation probability have positive correlations in the low bias range.

The reaction probability in molecule/surface systems is closely associated with the excited-state lifetimes [22, 26, 55, 56], which were generally measured by time-resolved photoemission or optical techniques [57-60]. Although the time resolution can be achieved in those measurements, spatial resolution at atomic level is difficult to achieve. A recent study showed that the proximity of STM tip suppresses the reaction probability by reducing the excited-state lifetime [22], suggesting the potential of STM to measure and control the coherent dynamics of excited carriers at the molecule/solid interface. Nevertheless, the excited-carrier lifetime was only estimated qualitatively. Here we quantitatively correlate the lower reaction probability of HS on Au(111) to the reduction of excited-state lifetimes. The lifetimes of injected electrons and the timescale of chemical reactions induced by inelastic electrons can therefore be measured. Hence, the STM technique and time-dependent *ab initio* NAMD simulations may be widely extended to understand the coherent dynamics of injected-electron induced chemical reactions on surfaces.

Acknowledgements

We thank Prof. Sheng Meng from IOP for the useful discussion about the DFT calculations, and Prof. Andrew Wee from NUS for his help about analysis of experimental data. This work was supported by the MOST of China (grants nos. 2016YFA0202301, 2017YFA0204904, 2018YFE0202700, 2016YFA0200604, 2016YFA0300904,), the NSF of China (grants nos. 11761141013, 11674366, 11674368, 11620101003, 11704363), the Beijing Natural Science Foundation (grants no. Z180007), and the Strategic Priority Research Program of the Chinese Academy of Sciences (grant no. XDB07010200, XDB30000000).

Reference

[1] B. C. Stipe, M. A. Rezaei, and W. Ho, Phys. Rev. Lett. **81**, 1263 (1998).

[2] B. C. Stipe, M. A. Rezaei, and W. Ho, Science **279**, 1907 (1998).

[3] T. Komeda, Y. Kim, M. Kawai, B. N. J. Persson, and H. Ueba, Science **295**, 2055 (2002).

[4] Y. Sainoo, Y. Kim, T. Okawa, T. Komeda, H. Shigekawa, and M. Kawai, Phys. Rev. Lett. **95**, 246102 (2005).

[5] J. Oh, H. Lim, R. Arafune, J. Jung, M. Kawai, and Y. Kim, Phys. Rev. Lett. **116**, 056101 (2016).

[6] J. Mielke, J. Martínez-Blanco, M. V. Peters, S. Hecht, and L. Grill, Phys. Rev. B 94, 035416 (2016).

[7] A. Shiotari, T. Odani, and Y. Sugimoto, Phys. Rev. Lett. **121**, 116101 (2018).

[8] Y. Kim, T. Komeda, and M. Kawai, Phys. Rev. Lett. **89**, 126104 (2002).

[9] M. Ohara, Y. Kim, S. Yanagisawa, Y. Morikawa, and M. Kawai, Phys. Rev. Lett. **100**, 136104 (2008).

[10] H. J. Shin, J. Jung, K. Motobayashi, S. Yanagisawa, Y. Morikawa, Y. Kim, and M. Kawai, Nat. Mater. **9**, 442 (2010).

[11] B. C. Stipe, M. A. Rezaei, and W. Ho, Phys. Rev. Lett. **78**, 4410 (1997).

[12] S. Gao, M. Persson, and B. I. Lundqvist, Phys. Rev. B **55**, 4825 (1997).

[13] S. G. Tikhodeev, and H. Ueba, Surf. Sci. **587**, 25 (2005).

[14] S. G. Tikhodeev, and H. Ueba, Phys. Rev. Lett. **102**, 246101 (2009).

[15] T. Frederiksen, M. Paulsson, and H. Ueba, Phys. Rev. B **89,** 035427 (2014).

[16] H. Gawronski, K. Morgenstern, and K. H. Rieder, Eur. Phys. J. D **35**, 349 (2005).

[17] J. Lee, D. C. Sorescu, and X. Deng, J. Am. Chem. Soc. **133**, 10066 (2011).

[18] S. Tan, Y. Zhao, J. Zhao, Z. Wang, C. Ma, A. Zhao, B. Wang, Y. Luo, J. Yang, and J. Hou, Phys. Rev. B **84**, 155418 (2011).

[19] T. Kudernac, N. Ruangsupapichat, M. Parschau, B. Maciá, N. Katsonis, S. R. Harutyunyan, K. H. Ernst, and B. L. Feringa, Nature (London) **479**, 208 (2011).

[20] L. Lauhon, and W. Ho, Surf. Sci. **451,** 219(2000).

[21] B. Jiang, D. Xie, and H. Guo, Chem. Sci. **4**, 503 (2013).

[22] K. R. Rusimova, R. M. Purkiss, R. Howes, F. Lee, S. Crampin, and P. A. Sloan, Science **361**, 1012 (2018).

[23] J. I. Pascual, N. Lorente, Z. Song, H. Conrad , and H. P. Rust, Nature (London) **423** (6939), 525 (2003).

[24] K. Motobayashi, Y. Kim, H. Ueba, and M. Kawai, Phys. Rev. Lett. **105**, 076101 (2010).

[25] K. Motobayashi, Y. Kim, R. Arafune, M. Ohara, H. Ueba, and M. Kawai, J. Chem. Phys. **140**, 194705 (2014).

[26] W. Paul, K. Yang, S. Baumann, N. Romming, T. Choi, C. P. Lutz, and A. J. Heinrich, Nat. Phys. **13**, 403 (2016).

[27] See Supplemental Material for details of experimental and calculational methods, as well as detailed calculated data. which includes Refs. [28–42]

[28] G. Kresse, and J. Hafner, Phys. Rev. B **47**, 558 (1993).

[29] G. Kresse, and J. Furthmüller, Phys. Rev. B **54**, 11 169 (1996).

[30] S. Grimme, J. Antony, S. Ehrlich, and H. Krieg, J. Chem. Phys. **132**, 154104 (2010).

[31] S. Grimme, S. Ehrlich, and L. Goerigk, J. Comput. Chem. **32**, 1456 (2011).

[32] J. P. Perdew, K. Burke, and M. Ernzerhof, Phys. Rev. Lett. **77**, 3865 (1996).

[33] G. Kresse, and D. Joubert, Phys. Rev. B **59**, 1758 (1999).

[34] G. Henkelman, B. P. J Uberuaga, and H. Jónsson, J. Chem. Phys. **113**, 9901 (2000).

[35] L. Qi, X. Qian, and J. Li, Phys. Rev. Lett. **101**, 146101 (2008).

[36] J. Behler, B. Delley, S. Lorenz, K. Reuter, and M. Scheffler, Phys. Rev. Lett. **94**, 036104 (2005).

[37] Q. Z. Zheng, J. Zhao, http://staff.ustc.edu.cn/~zhaojin/code.html

[38] X. Meng, J. Guo, J. Peng, J. Chen, Z. Wang, J. Shen, X. Li, E. Wang, and Y. Jiang, Nat. Phys. **11**, 235 (2015).

[39] A. J. H. McGaughey and J. M. Larkin, Annu. Rev. Heat Transfer **17**, 49 (2014).

[40] S. P. Rittmeyer, J. Meyer, J. I. Juaristi, and K. Reuter, Phys. Rev. Lett. **115**, 046102 (2015).

[41] D. Novko, M. Blanco-Rey, J. I. Juaristi, and M. Alducin, Phys. Rev. B **92**, 201411 (2015).

[42] I. Lonc□arić, M. Alducin, J. I. Juaristi, and D. Novko, J. Phys. Chem. Lett. **10**, 1043 (2019).

[43] H. F. Prest, W. B. Tzeng, J. M. Brom, Jr., and C. Y. Ng, J. Am. Chem. Soc. **105**, 7531 (1983).

[44] J. H. Chang, A. Huzayyin, K. Lian, and F. Dawson, Phys. Chem. Chem. Phys. **17** , 588 (2015).

[45] X. Zhang, Y. Tang, S. Qu, J. Da, and Z. Hao, ACS Catal. **5**, 1053 (2015).

[46] A. J. Leavitt, T. P. Beebe, and Jr. Surf. Sci. **314**, 23 (1994).

[47] P. N. Abufager, P. G. Lustemberg, C. Crespos, and H. F. Busnengo, Langmuir **24**, 14022 (2008).

[48] N. Liu, X. Y. Wang and Y. L. Wan, J. Theor. Comput. Chem. **13**, 1450065 (2014).

[49] D. R. Alfonso, Surf. Sci. **602**, 2758 (2008).

[50] H. Sellers, Surf. Sci. **294**, 99 (1993).

[51] D. Šestović, and M. Šunjić , Solid State Commun. **98**, 375 (1996).

[52] D. Šestović, L. Marušić, and M. Šunjić, Phys. Rev. B **55**, 1741 (1997).

[53] H. J. Lee, and W. Ho, Science **286**, 1719 (1999).

[54] Y. Kim, K. Motobayashi, T. Frederiksen, H. Ueba and M. Kawai, Prog. Surf. Sci., **90**, 85 (2015)

[55] P. Saalfrank, G. Boendgen, C. Corriol, and T. Nakajima, Faraday Discuss. **117**, 65 (2000).

[56] J. Repp, G. Meyer, F. E. Olsson, and M. Persson, Science **305**, 493 (2004).

[57] K. Onda, B. Li, J. Zhao,K. D. Jordan, J. Yang, and H. Petek, Science **308**, 1154 (2005).

[58] B. Li, J. Zhao, K. Onda, K. D. Jordan, J. Yang, and H. Petek, Science **311**, 1436 (2006).

[59] J. T. Yates, and H. Petek, Chem. Rev. **106**, 4113 (2006).

[60] H. Petek, and J. Zhao, Chem. Rev. **110**, 7082 (2010).

Figures

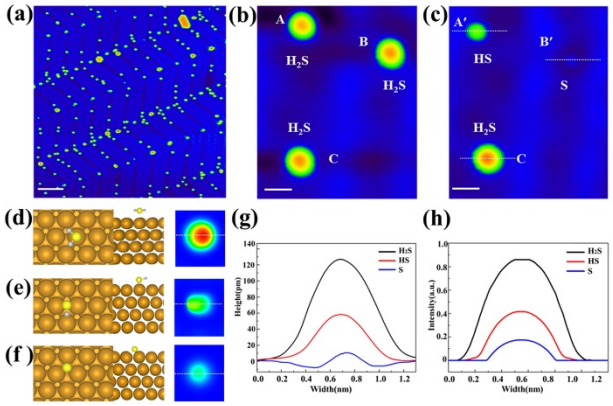

Figure 1. (a) STM image of 0.01 ML H_2S molecules adsorbed on Au(111) surface. Scale bar: 10 nm. (b) STM image of isolated H_2S molecules marked by A, B, C. (c) STM image of same area as (b) after applying pulses of -1.0 V with tunneling currents of 0.8 nA on molecule A and B, which are dissociated to HS (A') and S (B'), respectively. Scale bar: 1 nm. The scanning parameters of (a-c): V_{tip} = -100 mV, I = 100 pA. (d-f) The calculated results of single H_2S, HS, and S on Au(111), respectively. The left and middle panels are top and side view of relaxed structural models, in which the yellow, gray and gold balls represent S, H and Au atoms, respectively. The right panels are simulated STM images. (g, h) Line profiles along dotted lines in (c) and simulated H_2S, HS molecule and S atom images at -100 mV.

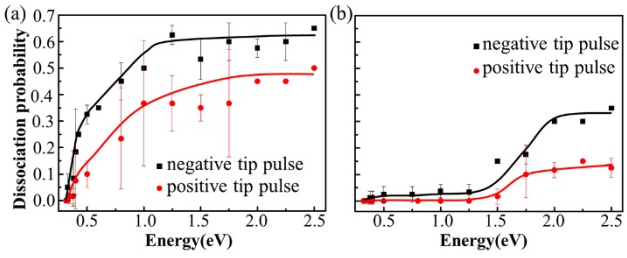

Figure 2. (a, b) The dissociation probability of isolated H_2S and HS on Au(111) surface induced by tip bias pulses, respectively. The black (red) lines indicate negative (positive) tip pulses applied on molecules. The probabilities are derived from the ratio of the number of dissociated molecules to the total number of trials (> 100

times) after pulsing with certain bias, as well as the constant tunneling current of 0.8 nA and pulse duration of 100 ms.

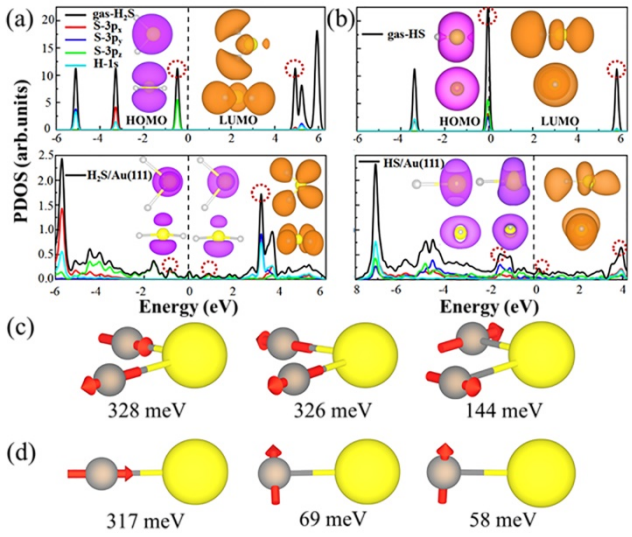

Figure 3. (a) PDOS of H_2S in gas phase (top panel) and on Au surface (bottom panel). (b) PDOS of HS in gas phase (top panel) and on Au surface (bottom panel). The vertical black dashed lines denote the Fermi level. The insets visualize the spatial distribution of the main DOS peaks depicted by red dashed circles near to Fermi level. (c, d) Illustration of the vibrational modes of H_2S and HS on Au surface, respectively. For a clear view, the Au(111) surface is hidden.

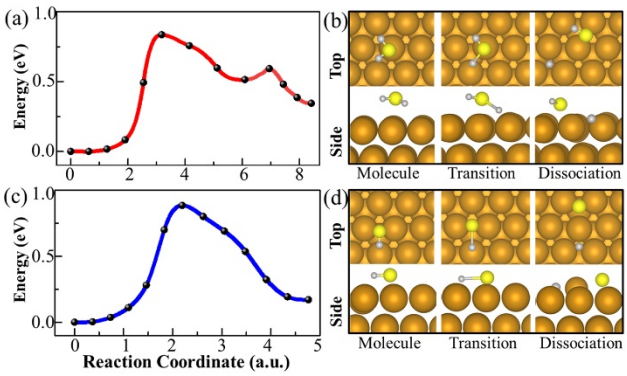

Figure 4. Reaction energy profile and atomic structure models along the reaction path of (a, b) an H_2S on Au(111) dissociates into HS+H, (c, d) HS monomer on Au(111) with H+S dissociated products.

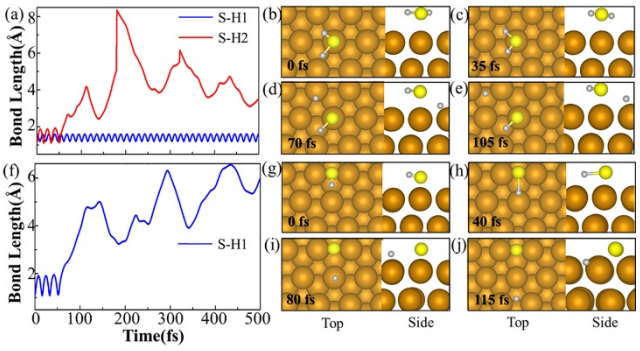

Figure 5. The time-dependent HS bond length evolutions in a 500 fs AIMD simulation for (a) H_2S molecule on Au surface and (f) HS on Au. The computed trajectories of H-S bond breaking in (b-e) isolated H_2S molecule and (g-j) isolated HS adsorbed on Au(111).

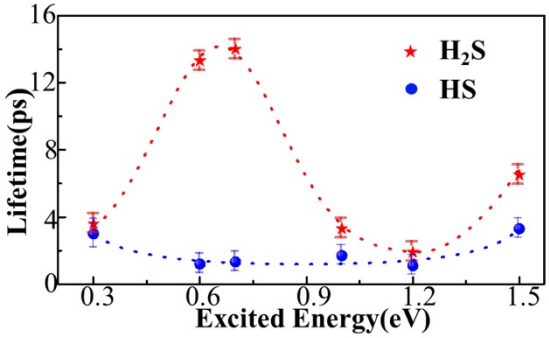

Figure 6. The lifetime of an excited-state electron initially generated via an IET process of H_2S and HS molecule on Au(111) with different initial energies at 100 K. The red and blue dotted lines are fits to the calculated data points.